

Binghamton University

## The Open Repository @ Binghamton (The ORB)

---

Undergraduate Honors Theses

Dissertations, Theses and Capstones

---

Spring 5-8-2020

### D-Glucose-6-phosphate stimulates SagS-dependent biofilm formation in *Pseudomonas aeruginosa*

Madison Gowett

*Binghamton University--SUNY*, [mgowett1@binghamton.edu](mailto:mgowett1@binghamton.edu)

Follow this and additional works at: [https://orb.binghamton.edu/undergrad\\_honors\\_theses](https://orb.binghamton.edu/undergrad_honors_theses)

 Part of the [Biology Commons](#)

---

#### Recommended Citation

Gowett, Madison, "D-Glucose-6-phosphate stimulates SagS-dependent biofilm formation in *Pseudomonas aeruginosa*" (2020). *Undergraduate Honors Theses*. 2.  
[https://orb.binghamton.edu/undergrad\\_honors\\_theses/2](https://orb.binghamton.edu/undergrad_honors_theses/2)

This Thesis is brought to you for free and open access by the Dissertations, Theses and Capstones at The Open Repository @ Binghamton (The ORB). It has been accepted for inclusion in Undergraduate Honors Theses by an authorized administrator of The Open Repository @ Binghamton (The ORB). For more information, please contact [ORB@binghamton.edu](mailto:ORB@binghamton.edu).

**D-Glucose-6-Phosphate Stimulates SagS-Dependent Biofilm Formation in *Pseudomonas aeruginosa***

By:

Madison Gowett


Advisor:

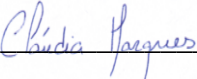
Karin Sauer, PhD


THESIS

Submitted in partial fulfillment of the requirements for  
Distinguished Independent Work in Biology  
Binghamton University  
State University of New York  
2020

Accepted in partial fulfillment of the requirements for  
Distinguished Independent Work in Biology  
Binghamton University  
State University of New York  
2020

Dr. Karin Sauer \_\_\_\_\_  \_\_\_\_\_ May 8, 2020  
Department of Biological Sciences

Dr. Cláudia Marques \_\_\_\_\_  \_\_\_\_\_ May 8, 2020  
Department of Biological Sciences

Dr. Susan Bane \_\_\_\_\_  \_\_\_\_\_ May 8, 2020  
Department of Chemistry

**Table of Contents**

**Abstract**.....5

**Introduction**.....6

**Materials and Methods**.....10

**Results**.....13

**Discussion**.....24

**References**.....29

## Tables and Figures

Figure 1. The system by which SagS regulates biofilm formation and antimicrobial tolerance independently of each other.....	8
Table 1. List of strains and plasmids used in this study.....	12
Table 2. Oligonucleotides used in this study.....	12
Figure 2. Effects of Mn <sup>2+</sup> on attachment.....	14
Figure 3. Effect of Mn <sup>2+</sup> on biofilm formation.....	15
Figure 4. Quantification of biofilm formation in the absence or presence of Mn <sup>2+</sup> .....	16
Figure 5. Identification of compounds that enhance attachment in a SagS-dependent way via Biolog screening.....	17
Figure 6. Effect of selected compounds on attachment.....	18
Figure 7. Dose-dependent effect of D-glucose-6-phosphate on attachment.....	19
Figure 8. Effect of D-glucose-6-phosphate on biofilm formation.....	20
Figure 9. Quantification of biofilm formation in the absence or presence of D-glucose-6-phosphate.....	21
Figure 10. Gene expression of biofilm marker genes.....	23

## ABSTRACT

The SagS protein is a two-component regulatory system in *Pseudomonas aeruginosa* that works to independently regulate biofilm formation and antibiotic tolerance. Previous work found that these two pathways are controlled by two distinct sets of amino acids within the sensory domain of SagS that are thought to be potential ligand binding sites. Despite the extensive research done on the structure and function of SagS, the signals that activate this protein have yet to be identified. In this study we aimed to identify ligands that stimulate SagS-dependent biofilm formation. To do this we utilized  $\Delta sagS$  mutants, one harboring wild-type *sagS* under the control of its native promoter and the other harboring the empty vector, attachment assays and COMSTAT analysis. Initially, we found that  $Mn^{2+}$  stimulates SagS-dependent attachment, but not SagS-dependent biofilm formation. While we ultimately identified D-glucose-6-phosphate as a ligand that enhances SagS-dependent biofilm formation. These findings provide a better understanding of how SagS works to control biofilm formation in *P. aeruginosa* and points to potential new method for treating *P. aeruginosa* infections.

## INTRODUCTION

Biofilms are communities of bacteria attached to a surface enmeshed in a self-produced protective matrix of extracellular polymeric substance (EPS) (1). With the heightened tolerance of biofilm associated cells and the protective nature of the EPS, biofilms are up to 1000x more resistant to antibiotics than their planktonic counterpart (2–4). These characteristics make most modern biofilm infection treatments unsuccessful, and with biofilms accounting for 80% of all chronic infections makes these communities especially dangerous to human health (5). Biofilms are the main mode of bacterial growth and are found everywhere, they can form on a number of biotic and abiotic surfaces in healthcare settings including contacts, medical implants and wounds (6–11). The Gram-negative bacterium *P. aeruginosa* is a common biofilm forming microbe that is an important human opportunistic pathogen as it has been associated with a number of chronic infections (12). *P. aeruginosa* biofilms are one of the main causes of persistent infections associated with cystic fibrosis and burn wounds (13–15).

The propensity of bacteria to form a biofilm is directly influenced by a number of environmental stimuli (16). These cues can be mechanical, such as the presence of a surface for bacteria to attach to or shear stress (16, 17). Other stimuli can be chemical and include anything from changes in nutrient levels, pH, osmolarity or extracellular small molecule concentrations (16, 18–22). Bacteria have different ways to sense these cues to then switch to a sessile lifestyle. One of the main ways bacteria can sense and respond to external signals is through two-component regulatory systems. These systems work to transduce signals inside the cell through the sensory domain of a membrane associated histidine kinase first sensing the signal and then phosphorylating a cytoplasmic response regulator or receiver (23). This results in the signal being transmitted throughout the cell through a series of phosphorylation cascades that eventually result in changes

in transcriptional control, enzymatic activities, or protein-protein interactions to bring about an adaptive response in the bacterium (24–26).

One of the various mechanisms by which *P. aeruginosa* forms a biofilm is through the control of the two-component regulatory protein SagS, which regulates the transition from planktonic to biofilm lifestyle and a switch to heightened antimicrobial tolerance. (27). SagS is composed of three domains, an N-terminal periplasmic sensory domain (HmsP), a histidine kinase (HisKA) domain and a C-terminal response regulator receiver (Rec) domain (27–30). This two-component hybrid has been found to control biofilm formation and antibiotic tolerance through two independent systems, with the inactivation of *sagS* leading to biofilms being arrested in irreversible attachment and biofilm cells being susceptible to antimicrobials (27, 29, 31). SagS is unique from other dual function proteins in that its domain makeup allows its two functions to be controlled by distinct domains within the protein (28). Figure 1 depicts how SagS is able to independently regulate biofilm formation and antibiotic tolerance (32). SagS first senses a signal, then signal perception results in phosphorylation of the histidine in the HisKA domain which then activates a phosphoryl transfer to an aspartic acid in the Rec domain, this transfer is controlled by a conformational change in the HAMP domain (28, 29). The phosphoryl group is subsequently transferred from SagS to BfiS to activate biofilm formation (27, 28, 33, 34). In contrast, SagS contributes to antibiotic tolerance through sensing a cue through the HmsP sensory domain, which then indirectly activates transcriptional regulator BrlR by increasing cyclic-di-GMP (c-di-GMP) levels in the cell (27, 28, 31, 35). High levels of c-di-GMP, an intracellular second messenger molecule, correlates with biofilm formation and reduced levels of this molecule are associated with a planktonic lifestyle (36). High levels of c-di-GMP increases expression of *brlR* and activates



BrIR which then binds to DNA and controls the expression of different ABC transporters and drug efflux pumps (27, 31, 35, 36).

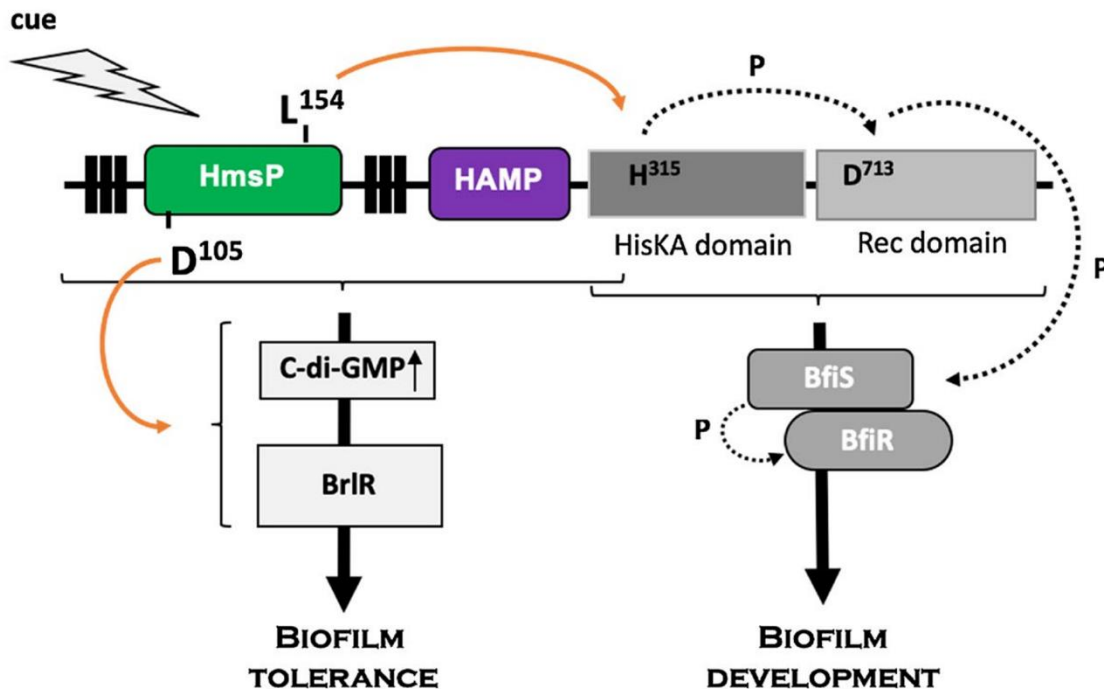


**Figure 1. The system by which SagS regulates biofilm formation and antimicrobial tolerance independently of each other.** When sensing an external cue through the sensory domain of the periplasmic HmsP domain, Sags induces biofilm formation by transducing the signal to the HisKA domain through changes in the HAMP domain. This results in a phosphotransfer from the histidine in the HisKA at position 315 to the aspartic acid in the Rec domain at position 713. This then leads to the phosphorylation of BfiS, which starts a subsequent phosphorylation cascade resulting in biofilm development. In contrast, after sensing a signal SagS controls antibiotic tolerance by increasing c-di-CMP levels which indirectly controls gene expression of BrIR. L154 represents a key residue in the set of amino acids responsible for sensing cues that lead to biofilm formation while residue D105 is a part of the set of amino acids that play a key role in regulating tolerance. HmsP, N-terminal periplasmic sensory domain. HAMP, HAMP domain. HisKA, histidine kinase domain. Rec, C-terminal response regulator receiver. The three vertical lines represent the transmembrane spanning helices. Figure obtained from: Dingemans J, Al-Feghali RE, Lau GW, Sauer K. 2019. Controlling chronic *Pseudomonas aeruginosa* infections by strategically interfering with the sensory function of SagS. *Mol Microbiol* 111:1211–1228.

SagS is able to sense external cues through its sensory HmsP domain, where it can go on to activate biofilm formation or antimicrobial tolerance. Previous works have found that within the HmsP domain there are distinct sets of amino acids that contribute to the regulation of biofilm formation and tolerance (29). When residues in these sets of amino acids are mutated one of the

sensory functions of SagS is inhibited. When D105 was mutated, biofilms had increased susceptibility to antibiotics while mutation of L154 caused *P. aeruginosa* to be unable to form biofilms (Figure 1). This shows that L154 belongs to the set of amino acids that sense cues that activate biofilm formation and D105 belongs to the group of residues that are part of the regulatory circuit that controls heightened tolerance. The sensory function of these two groups of amino acids indicate that they are part of what are thought to be ligand binding interaction or signal relay sites (29).

While previous works have studied the function and structure of the SagS protein in depth, the signals that activate SagS have yet to be identified. In this study we aimed to identify potential ligands that interact with SagS to induce biofilm formation and antibiotic tolerance in *P. aeruginosa*. To address this, we utilized  $\Delta sagS$  mutants, one harboring an empty CTX plasmid and the other complemented with wild-type *sagS* expressed under its native reporter to determine the impacts different molecules have on SagS-dependent attachment and biofilm formation through attachment assays and microscopy. Identifying potential signals that activate SagS will lead to a better understanding of biofilm formation and antibiotic resistance in *P. aeruginosa* and could point to new methods for biofilm control.

## **MATERIALS AND METHODS**

**Bacterial strains, plasmids, and culture conditions.** All bacterial strains and plasmids are listed in Table 1. Overnight cultures were grown in Lennox Broth (LB) at 37°C under shaking conditions (220 rpm).

**Screening of compounds using Biolog system.** To identify potential molecules that would affect attachment in a SagS-dependent way, a high throughput screening was performed using Phenotyping Microarrays (PM) plates (Biolog Inc., Hayward, CA) containing various carbon and nitrogen sources as well as osmolytes. This allowed for the testing multiple compounds on one plate. For plates PM1-3 (containing carbon and nitrogen sources), overnight cultures were diluted 100-fold in inoculation fluid IF-0 (Biolog Inc., Hayward, CA) supplemented with 20 mM sodium succinate. Each well of the PM plate was filled with 100 µl of the diluted culture and incubated at 37°C for 24h with intermittent shaking at 220 rpm. In case of plate PM9 (osmolytes), overnights were first diluted 100-fold in inoculation fluid IF-0 and subsequently 200-fold in inoculation fluid IF-10 without the addition of sodium succinate. Similarly, the plates were incubated at 37°C for 24h while shaking. On day 2, the OD<sub>600nm</sub> was first determined, followed by removal of the culture medium and hence, non-attached cells. Each well was filled with 100 µl of 0.85% saline to which 25 µl of a 0.1% (wt/vol) crystal violet solution was added. Plates were incubated for 15 minutes while shaking at 37°C and washed 4 times with 100 µl of Nanopure water, air-dried, after which the remaining crystal violet was dissolved in 100 µl of 95% ethanol. Finally, the OD<sub>570nm</sub> was determined using a SpectraMax i3x plate reader (Molecular Devices).

**Attachment assays.** Overnight cultures of *P. aeruginosa* were diluted 100-fold in LB medium supplemented with or without 100  $\mu$ M  $MnCl_2$  or other compounds of interest to an  $OD_{600nm}$  of 0.025 and 200  $\mu$ l of the resulting dilution was added to each well of a 96-well plate followed by 24h of incubation at 37°C with continuous shaking at 220 rpm, Next, 50  $\mu$ l of a 0.1% (wt/vol) crystal violet solution was added to each well and plates were incubated for 15 min at 37°C while shaking. Plates were washed four times with 200  $\mu$ l of Nanopure water to remove non-attached cells and excess crystal violet and allowed to dry. Finally, the remaining crystal violet was resuspended in 200  $\mu$ l of 95% ethanol and the  $OD_{570nm}$  was determined. LB medium was utilized as a blank and was subtracted from all values.

**Biofilm formation.** For RNA extraction, biofilms were grown in a continuous flow reactor system with size 13 (1m in length) Masterflex silicone tubing (Cole Parmer) at a flow rate of 0.1 ml/min, as previously described using 20-fold-diluted LB medium (37–39). After 3 days biofilms were treated with or without 10mM D-glucose-6-phosphate under flowing conditions for 15 minutes, following treatment flow was turned off for 20 minutes before harvesting. To visualize and quantify biofilm formation, biofilms were grown in 24-well plates in 5-fold-diluted LB medium with or without 100  $\mu$ M  $MnCl_2$  or 10 mM D-glucose-6-phosphate, with the growth medium being exchanged every 12h as previously described (29). Confocal laser scanning microscopy (CLSM) images were acquired using a Leica TCS SP5 confocal microscope (Leica Microsystems, Inc., Wetzlar, Germany) and the LIVE/DEAD BacLight bacterial viability kit (Life Technologies, Inc.). Quantitative analysis of the confocal laser scanning microscope images of 24-well plate-grown biofilms was performed using COMSTAT (40).

**RNA isolation and qRT-PCR.** Biofilms grown in biofilm tube reactors were harvested by extrusion, with the cell paste being collected directly into 500  $\mu$ l of RNAProtect Bacteria Reagent (Qiagen), followed by RNA extraction as previously described (41). Genomic DNA was removed using 1  $\mu$ l of (2U/ $\mu$ l) Turbo DNase (Ambion) for 30 min and cDNA was prepared using the iScript Select cDNA synthesis kit (Biorad) starting from 1  $\mu$ g of total RNA. qRT-PCR was performed using the BioRad CFX Connect Real-Time PCR Detection System and SsoAdvanced SYBR Green Supermix (BioRad) with primers listed in Table 2. The *mreB* gene was used as a housekeeping gene. Fold changes were calculated using the Livak method (42). Melting curve analyses were performed to verify specific single product amplification.

**Statistical analysis.** Statistical differences between growth conditions and/or strains were determined using a one-way ANOVA, followed by a Dunnett's post-hoc test using Prism5 software (Graph Pad, La Jolla, CA, USA).

**Table 1. List of strains and plasmids used in this study.**

Strains	Relevant genotype or description	Source
<b>Strains</b>		
$\Delta$ <i>sagS</i> ::CTX	PAO1, $\Delta$ <i>sagS</i> harboring the empty pMini CTX vector, Tet <sup>R</sup>	Dingemans et al., 2019
$\Delta$ <i>sagS</i> ::CTX- <i>sagS</i>	PAO1, $\Delta$ <i>sagS</i> harboring chromosomal insertion of <i>sagS</i> under the control of the <i>P</i> <sub><i>sagS</i></sub> promoter at <i>attB</i> site, cured pMini CTX vector	Dingemans et al., 2019

**Table 2. Oligonucleotides used in this study.**

Oligonucleotide	Sequence
<i>mreB</i> _F	CTTCATCAACAAGGTCCACGA
<i>mreB</i> _R	GCTCTTCGATCAGGAACACC
<i>pelA</i> _F	GGTGCTGGAGGACTTCATC
<i>pelA</i> _R	GGATGGCTGAAGGTATGGC
<i>pslG</i> _F	CACGTAAGGGACTCTATCTGG
<i>pslG</i> _R	AGGAAGTCTTCCAGACCAC

## RESULTS

### Manganese stimulates SagS-dependent attachment but not biofilm formation

It has been previously proven that the SagS protein regulates both biofilm formation and heightened tolerance to antimicrobials in *P. aeruginosa* (27–29, 31). To test whether compounds activate SagS we utilized attachment assays as an initial quick and easy way to observe the impacts compounds have on biofilm formation. To determine whether compounds enhanced SagS-dependent biofilm formation we utilized two  $\Delta sagS$  mutant strains, one complemented with the wildtype *sagS* gene chromosomally expressed under its native promoter ( $\Delta sagS::CTX-sagS$ ) and a  $\Delta sagS$  mutant harboring an empty CTX vector ( $\Delta sagS::CTX$ ). This allowed us to observe the impacts each tested compound has on attachment in the absence of *sagS* gene expression. The first compound we tested was manganese ( $Mn^{2+}$ ) as previous studies have found that this compound, and other divalent cations, promote biofilm formation in other microbes and interacts with and activates a histidine kinase in *Bacillus subtilis* (43–45). Therefore, we tested the attachment of both strains by staining biofilms that were grown in the presence and absence of  $Mn^{2+}$  for 24-hours with crystal violet (CV). This allowed for the attached biofilm biomass to be quantified. In the presence of 100  $\mu M$  of  $Mn^{2+}$  there was a significant increase in attached biomass in  $\Delta sagS::CTX-sagS$  when compared to its untreated counterpart. There was no significant difference in attached biomass in treated and untreated  $\Delta sagS::CTX$  (Figure 2). These findings indicate  $Mn^{2+}$  enhances SagS-dependent attachment at 24 hours.

To visualize and quantify the impacts  $Mn^{2+}$  has on biofilm formation,  $\Delta sagS::CTX$  and  $\Delta sagS::CTX-sagS$  were grown for 3 days with or without  $Mn^{2+}$  and then imaged using confocal microscopy (29, 40). Following COMSTAT analysis we found that in the presence of 100  $\mu M$   $Mn^{2+}$  both  $\Delta sagS::CTX-sagS$  and  $\Delta sagS::CTX$  had a significant decrease in average biofilm

thickness and maximum thickness, while  $\Delta sagS::CTX-SagS$  had a significant decrease in total biomass and a significant increase in substratum coverage. While  $\Delta sagS::CTX$  had a significant increase in total biofilm biomass and substratum coverage when treated with  $Mn^{2+}$  (Figure 4). There was also a visible decrease in microcolony formation in both  $\Delta sagS::CTX-sagS$  and  $\Delta sagS::CTX$  in the presence of  $Mn^{2+}$  (Figure 3). While  $Mn^{2+}$  increases biofilm attachment in  $\Delta sagS::CTX-sagS$ , this divalent cation does not enhance SagS-dependent biofilm formation in *P. aeruginosa*, leading us to investigate other molecules as potential signals.

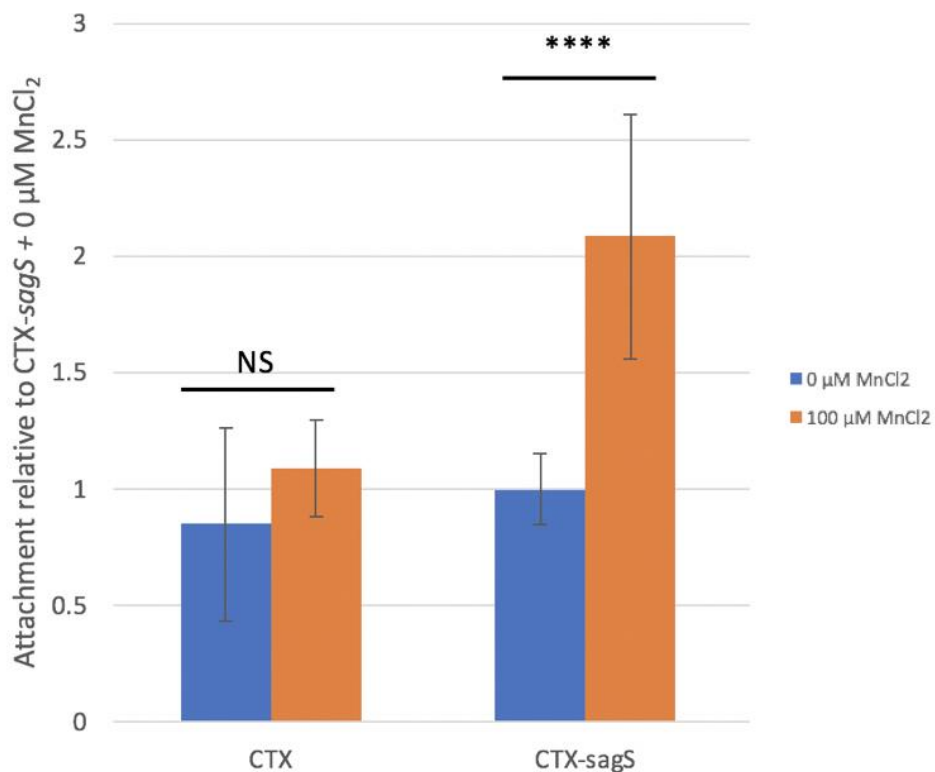


**Figure 2. Effects of  $Mn^{2+}$  on attachment.** Crystal violet staining of attached cells grown for 24h in LB medium was carried out with or without 100  $\mu M Mn^{2+}$ .  $Mn^{2+}$  significantly enhances attachment of  $\Delta sagS$  complemented with wild-type *sagS*, but not  $\Delta sagS$  harboring the empty CTX vector. All assays were repeated at least two times, with each repeat consisting of at least 6 technical replicates. Error bars denote standard deviation. \*\*\*\*,  $P < 0.0001$  indicates significantly different from untreated condition. NS, not significantly different.

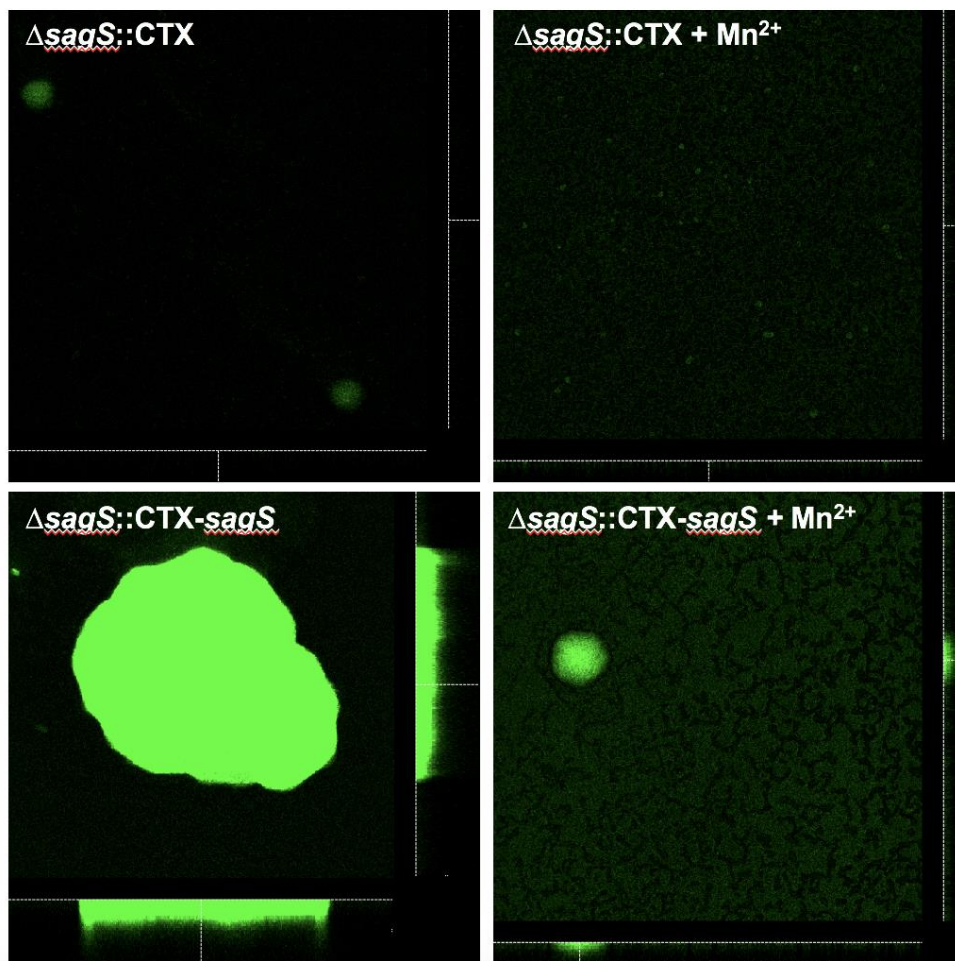


**Figure 3. Effect of  $Mn^{2+}$  on biofilm formation.** Biofilms of *P. aeruginosa*  $\Delta sagS$  harboring an empty CTX vector or complemented with wild-type *sagS* were grown in 24-well plates in 5-fold-diluted LB medium with or without  $100 \mu M Mn^{2+}$ , with the growth medium being exchanged every 12h as previously described. Confocal laser scanning microscopy (CLSM) images were acquired using a Leica TCS SP5 confocal microscope (Leica Microsystems, Inc., Wetzlar, Germany) and the LIVE/DEAD BacLight bacterial viability kit (Life Technologies, Inc.).



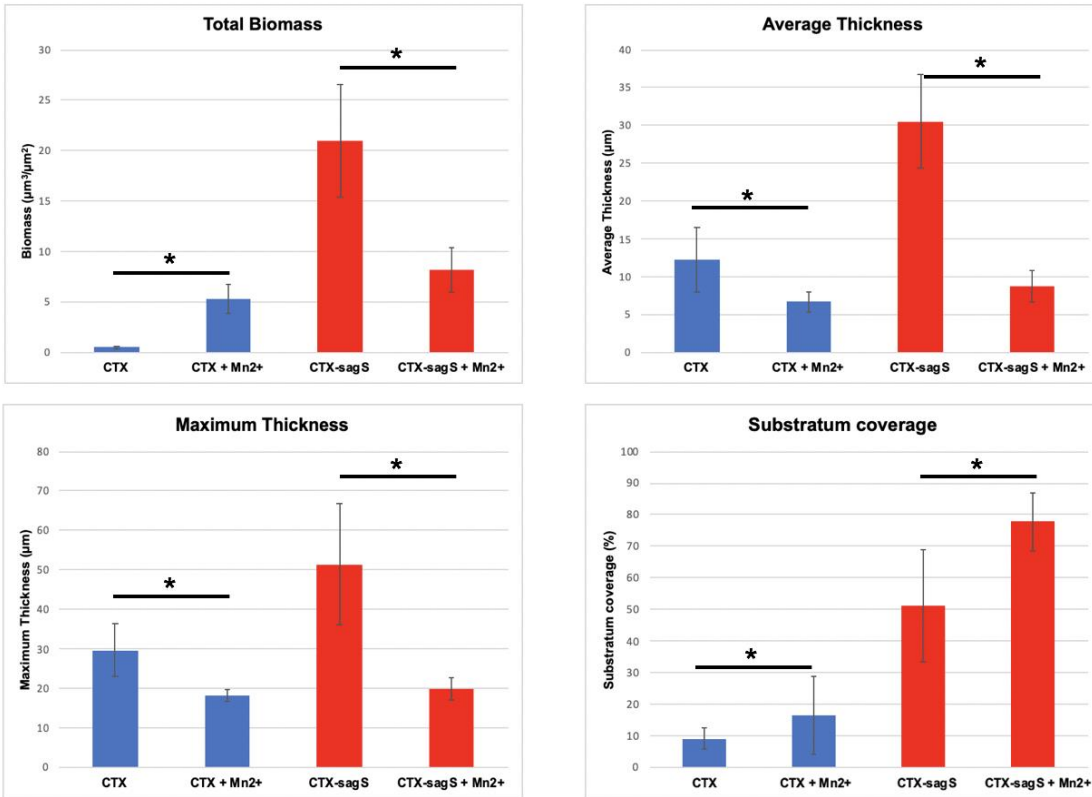


**Figure 4. Quantification of biofilm formation in the absence or presence of Mn<sup>2+</sup>.** COMSTAT analysis of Confocal laser scanning microscopy (CLSM) images acquired from biofilms of *P. aeruginosa*  $\Delta$ *sagS* harboring an empty CTX vector or complemented with wild-type *sagS* grown with or without 100  $\mu$ M Mn<sup>2+</sup>. All assays were repeated at least two times, with a minimum of 6 images being acquired. Error bars indicate standard deviation. \*, P < 0.05 indicates significantly different from untreated condition.

## Biolog Phenotyping Microarray Screen reveals compounds that stimulates SagS-dependent attachment

In order to perform a high throughput screen of potential compounds that impact SagS-dependent attachment PM plates containing various carbon sources, nitrogen sources and osmolytes were utilized. The attachment of both  $\Delta$ *sagS*::CTX-*sagS* and  $\Delta$ *sagS*::CTX in the presence and absence of each compound tested was quantified using CV staining at 24 hours. Figure 5 shows the compounds identified to have enhanced attachment in treated  $\Delta$ *sagS*::CTX-*sagS* but not  $\Delta$ *sagS*::CTX through the Biolog screenings. From those identified compounds D-glucose-6-phosphate (G6P), glycerol and  $\beta$ -methyl-D-galactosidase were further tested to quantify

their impacts on SagS-dependent attachment, as these compounds had a large increase in attachment of  $\Delta sagS::CTX-sagS$  compared to  $\Delta sagS::CTX$  (Figure 5). With G6P being the only compound identified to have enhanced attachment in treated  $\Delta sagS::CTX-sagS$  but not treated  $\Delta sagS::CTX$  (Figure 6). This indicated that G6P enhances SagS-dependent attachment.

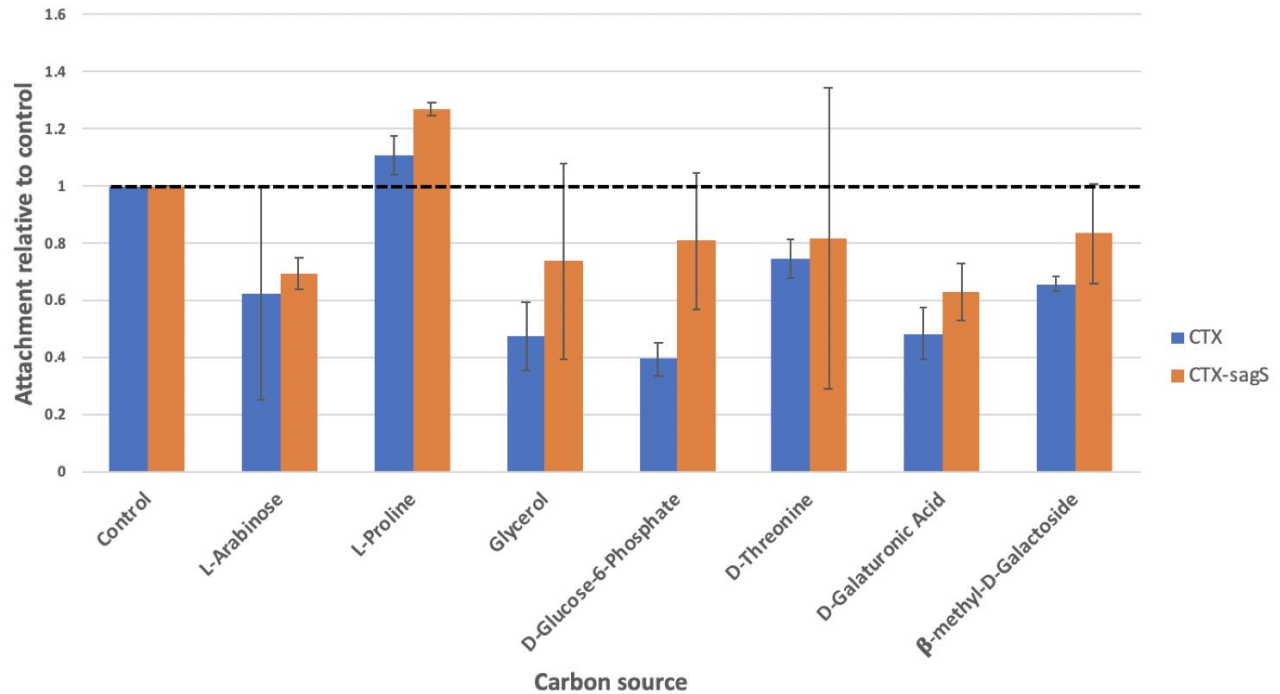


**Figure 5. Identification of compounds that enhance attachment in a SagS-dependent way via Biolog screening.** A high throughput screening was performed using Phenotyping Microarrays (PM) plates (Biolog Inc., Hayward, CA) containing various carbon and nitrogen sources as well as osmolytes. Each PM plate was filled with 100  $\mu$ l of a diluted overnight culture and incubated at 37°C for 24h with intermittent shaking at 220 rpm, followed by crystal violet staining. Finally, the OD<sub>570nm</sub> was determined using a SpectraMax i3x plate reader (Molecular Devices) and normalized to the OD<sub>600nm</sub> obtained after 24h of growth. Attachment was normalized to a control condition (without adding compounds other than sodium succinate as a carbon source for the plates containing minimal medium). Each compound was tested in biological duplicate with one well per assay.

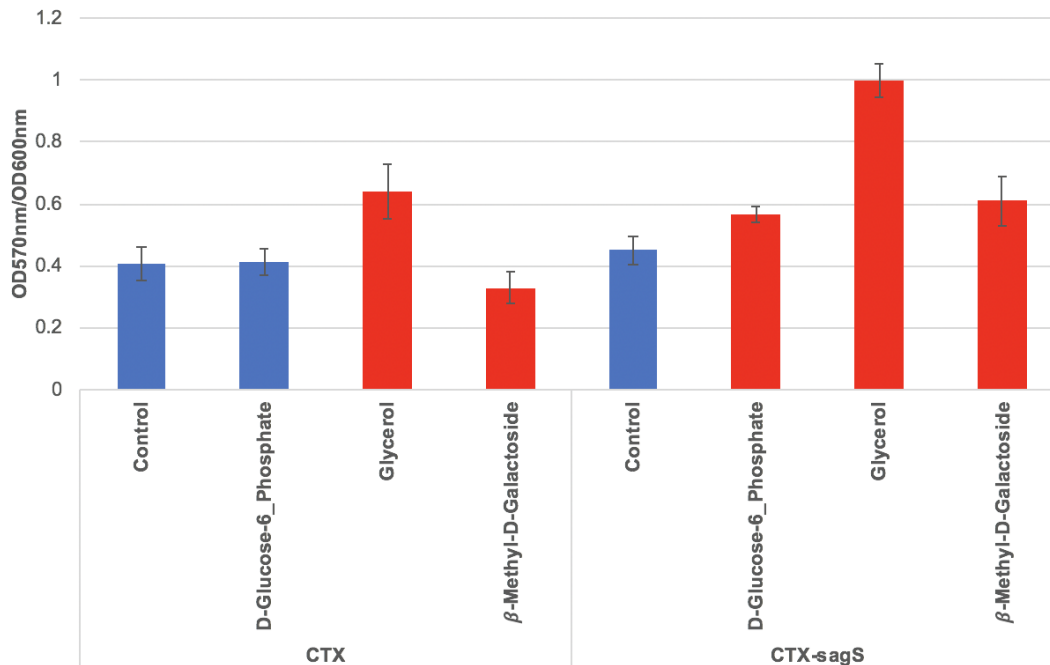


**Figure 6. Effect of selected compounds on attachment.** Compounds identified during the initial Biolog screening were further tested in regular 96-well plates. Overnight cultures of *P. aeruginosa* were diluted 100-fold in LB medium supplemented with the compound of interest to an OD<sub>600nm</sub> of 0.025 and 200  $\mu$ l of the resulting dilution was added to each well of a 96-well plate followed by 24h of incubation at 37°C with continuous shaking at 220 rpm. Next, 50  $\mu$ l of a 0.1% (wt/vol) crystal violet solution was added to each well and plates were incubated for 15 min at 37°C while shaking. Plates were washed four times with 200  $\mu$ l of Nanopure water to remove non-attached cells and excess crystal violet and allowed to dry. Finally, the remaining crystal violet was resuspended in 200  $\mu$ l of 95% ethanol and the OD<sub>570nm</sub> was determined and normalized to the OD<sub>600nm</sub>.

### D-Gucose-6-Phosphate enhances biofilm formation in a SagS-dependent way

To determine the dose-dependent effects of G6P on SagS-dependent attachment, both strains were grown in increasing concentrations of the compound for 24-hours. Attached cells were stained with CV to quantify attached biomass. We found that increasing concentrations of G6P increased biofilm attachment in  $\Delta sagS::CTX-sagS$  but not  $\Delta sagS::CTX$  (Figure 7). Results showed increasing concentrations of G6P increased SagS-dependent attachment in *P. aeruginosa*.

To observe and quantify the effects of G6P on biofilm formation, both strains were grown in the absence and presence of this compound for 3 days, imaged using confocal microscopy (Figure 8) and analyzed using COMSTAT (Figure 9). We found that 10mM of G6P had a

significant increase in total biomass and substratum coverage as well as increased microcolony formation in just  $\Delta sagS::CTX-sagS$  (Figure 8 and 9). Results indicate that G6P stimulates SagS-dependent biofilm formation.

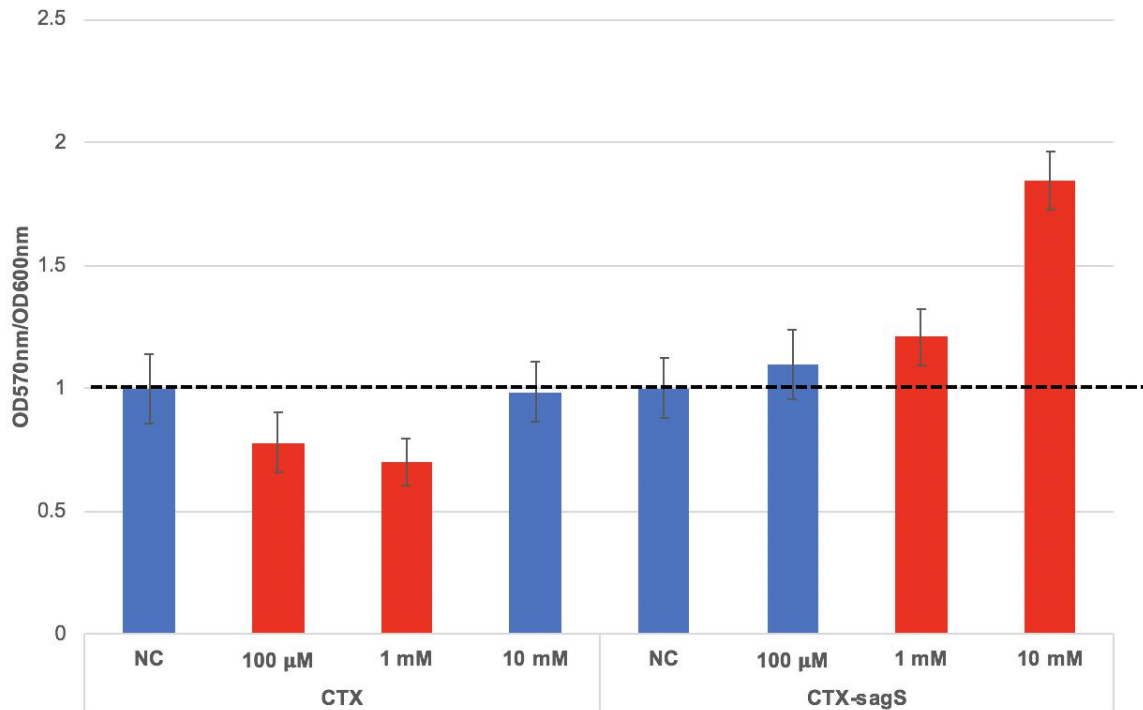


**Figure 7. Dose-dependent effect of D-glucose-6-phosphate on attachment.** An overnight culture of *P. aeruginosa*  $\Delta sagS$  harboring an empty CTX vector or complemented with wild-type *sagS* was diluted 100-fold in LB medium supplemented with increasing concentrations of D-glucose-6-phosphate to an OD<sub>600nm</sub> of 0.025 and 200  $\mu$ l of the resulting dilution was added to each well of a 96-well plate, followed by 24h of incubation at 37°C with continuous shaking at 220 rpm. Crystal violet staining was performed as previously described and the OD<sub>570nm</sub> was determined and normalized to the OD<sub>600nm</sub>.

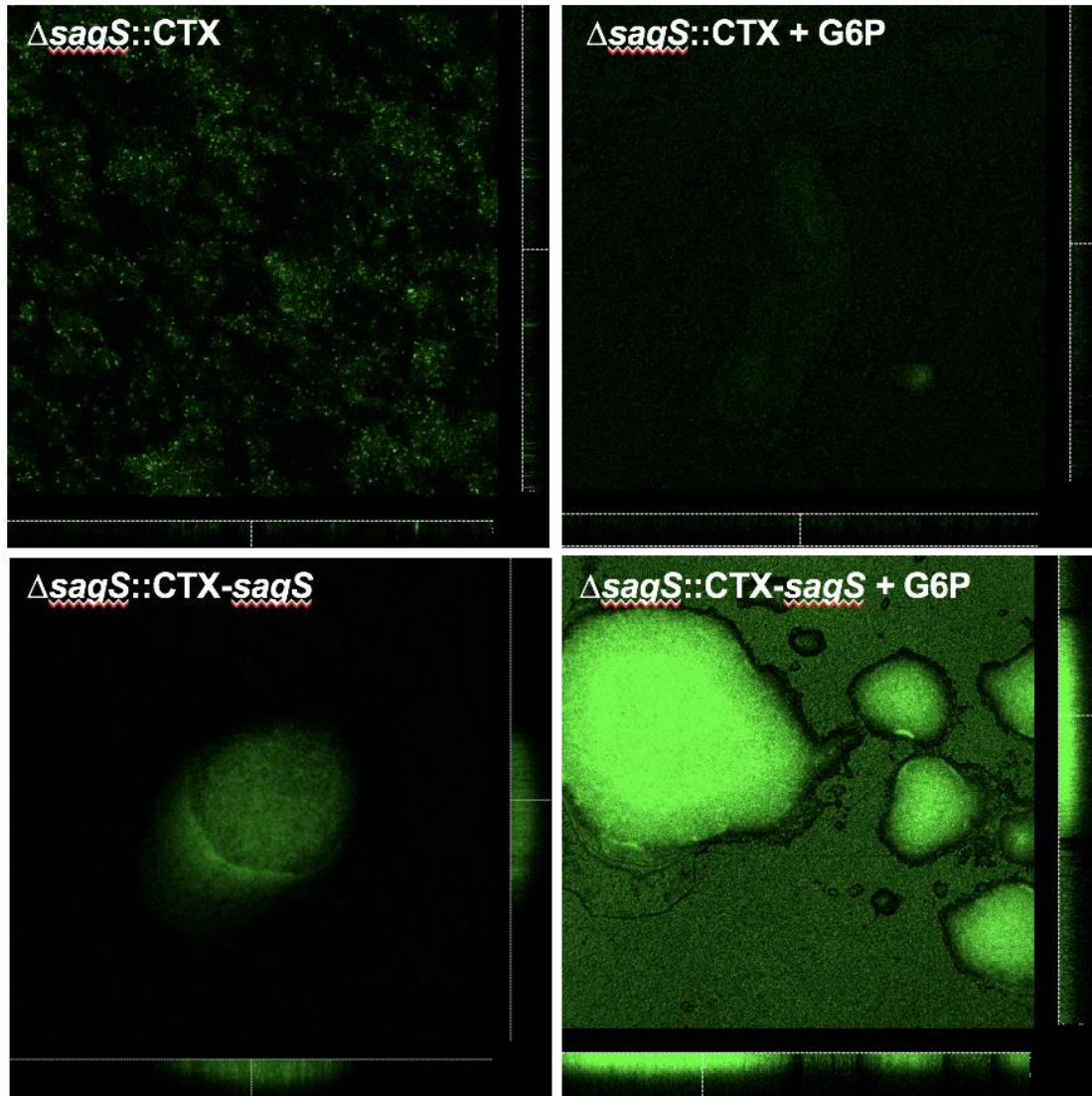


**Figure 8. Effect of D-glucose-6-phosphate on biofilm formation.** Biofilms of *P. aeruginosa*  $\Delta$ *sagS* harboring an empty CTX vector or complemented with wild-type *sagS* were grown in 24-well plates in 5-fold-diluted LB medium with or without 10 mM D-glucose-6-phosphate, with the growth medium being exchanged every 12h. Confocal laser scanning microscopy (CLSM) images were acquired using a Leica TCS SP5 confocal microscope (Leica Microsystems, Inc., Wetzlar, Germany) and the LIVE/DEAD BacLight bacterial viability kit (Life Technologies, Inc.). G6P, D-glucose-6-phosphate.

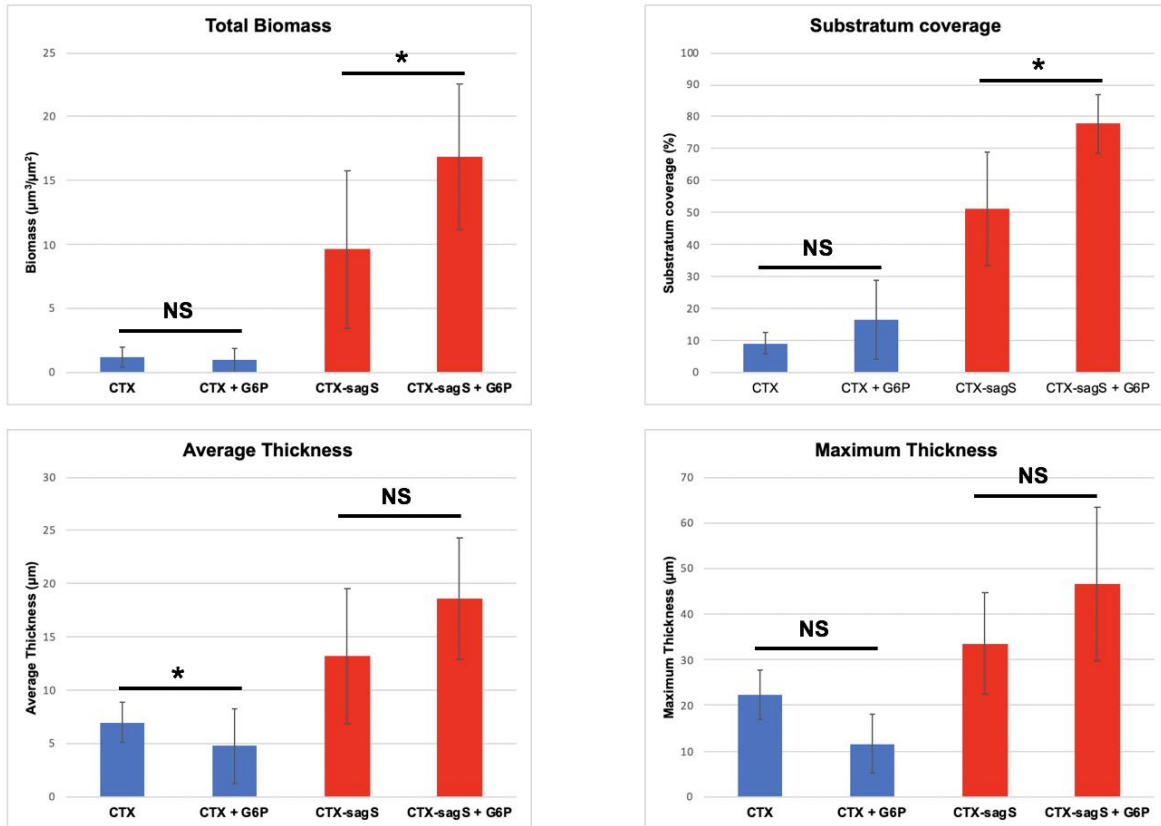


**Figure 9. Quantification of biofilm formation in the absence or presence of D-glucose-6-phosphate.** COMSTAT analysis of Confocal laser scanning microscopy (CLSM) images acquired from biofilms of *P. aeruginosa*  $\Delta sagS$  harboring an empty CTX vector or complemented with wild-type *sagS* grown with or without 10 mM D-glucose-6-phosphate. All assays were repeated at least two times, with a minimum of 6 images being acquired. Error bars indicate standard deviation. \*,  $P < 0.05$  indicates significantly different from untreated condition. NS, not significantly different. G6P, D-glucose-6-phosphate.

### D-glucose-6-phosphate enhances biofilm marker gene expression in *AsagS::CTX-sagS*

We next asked how G6P impacted biofilm marker gene expression in order to determine how this compound contributes to the biofilm phenotype in both mutants. It's been proven that gene expression changes in *P. aeruginosa* when planktonic cells transition to a sessile lifestyle (46). Biofilm marker genes play a role in allowing bacteria to form a biofilm and are found to be highly upregulated in biofilm cells. Looking at the expression of biofilms marker genes can further reveal whether G6P stimulates biofilm formation, with increased expression of these genes indicating enhanced biofilm formation. The two biofilm marker genes that we focused on were

*pelA* and *pslG*, with *mreB* acting as the housekeeper gene. Both of these genes help to promote biofilm formation by controlling exopolysaccharide production with *pelA* controlling glucose-rich extracellular matrix production and *pslG* controlling the synthesis of mannose-rich exopolysaccharides (47, 48). Looking at gene expression of biofilm marker genes in the presence of G6P can indicate how this molecule contributes to the biofilm phenotype and subsequently biofilm formation in both mutants. Based on the transcript abundance data obtained from one assay,  $\Delta sagS::CTX-sagS$  had a >2-fold upregulation in gene expression of both *pelA* and *pslG* demonstrated a 2-fold increase in transcript abundance in  $\Delta sagS::CTX-sagS$  biofilms when normalized to its untreated counterpart. While  $\Delta sagS::CTX$  had a >2-fold upregulation of *pelA* and a very small upregulation of *pslG* in the presence of G6P when normalized to its untreated counterpart. When comparing gene expression of treated  $\Delta sagS::CTX-sagS$  to treated  $\Delta sagS::CTX$  expression, G6P seemed to have the same impacts on gene expression of *pelA* in both strains. While G6P had a larger upregulation of *pslG* in  $\Delta sagS::CTX-sagS$  than in  $\Delta sagS::CTX$ , with the vector control having little change in expression of *pslG* in treated vs untreated conditions (Figure 10). In all results show that G6P had a similar impact on gene expression of *pelA* in both strains, while G6P only increased expression of *pslG* in just  $\Delta sagS::CTX-sagS$ . This supports that G6P enhances SagS-dependent biofilm formation by upregulating expression of biofilm marker *pslG* in just  $\Delta sagS::CTX-sagS$  and not in  $\Delta sagS::CTX$ .

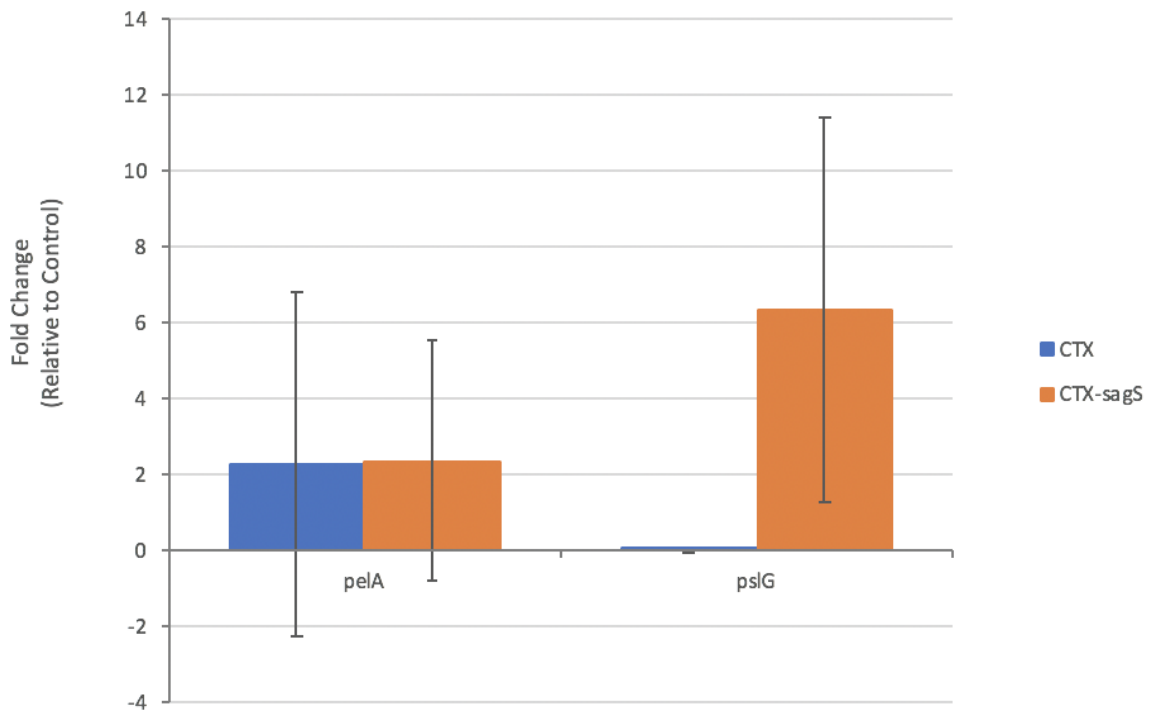


**Figure 10. Gene expression of biofilm marker genes.** RNA was extracted from 3-day old biofilms of *P. aeruginosa*  $\Delta sagS$  harboring an empty CTX vector or complemented with wild-type *sagS* grown with or without 10 mM D-glucose-6-phosphate to utilize for qRT-PCR. Gene expression was normalized to the control for each strain, with the control being the untreated condition of each strain, thus showing the fold change of treated relative to untreated biofilms. The housekeeper utilized in this assay was *mreB*. D-glucose-6-phosphate had similar impacts on gene expression of *pelA* for both strains while this compound had a large increase in expression of *pslG* in just  $\Delta sagS::CTX-sagS$ . This assay was performed once using technical duplicates. Error bars indicate standard deviation.



## DISCUSSION

Bacteria, like *P. aeruginosa*, can form biofilms by sensing external stimuli. This switch from planktonic to a sessile biofilm is controlled through different regulatory processes such as quorum sensing, cyclic-di-GMP levels and two-component regulatory systems (49–52). In order for bacteria to first attach and then progress through the stages of biofilm development the bacterium must first sense some sort of external cue (27). This signal is first detected by a number of different sensory proteins within *P. aeruginosa*, including the two-component system SagS (28, 53, 54). This protein senses external signals through distinct sets of amino acids within its periplasmic sensory HmsP domain and, because of its domain composition, works to independently control the switch from planktonic to biofilm growth and heightened antimicrobial tolerance in *P. aeruginosa* (27–30, 34). While extensive research has been done on the SagS protein the ligands responsible for activating it has yet to be identified.

In this study we worked to identify potential ligands responsible for activating SagS by utilizing  $\Delta sagS::CTX-sagS$ , a  $\Delta sagS$  mutant complemented with wildtype  $sagS$  under its native promoter and  $\Delta sagS::CTX$ , a  $\Delta sagS$  mutant harboring an empty CTX plasmid and attachment assays. This allowed us to quickly observe how different compounds impact SagS-dependent biofilm formation. The first compound we investigated was  $Mn^{2+}$ , as it has been found that in *B. subtilis*  $Mn^{2+}$  increases biofilm formation through the activation of the KinD histidine kinase by interacting with its Cache domain, a common extracellular small-molecule sensor in bacteria (44, 54). Previous findings have suggested that the HmsP sensory domain of SagS may adopt a similar shape to the Cache domain and due to the potential similarities in structure, investigating this divalent cation seemed like a promising start (29). Attachment assays revealed that  $Mn^{2+}$  significantly increased SagS-dependent biofilm formation at 24 hours, as attachment was enhanced

in  $\Delta sagS::CTX-sagS$  but not  $\Delta sagS::CTX$  (Figure 2). Thus, indicating this divalent cation may interact with SagS during initial attachment but further analysis revealed that  $Mn^{2+}$  did not enhance biofilm formation in 3-day old biofilms. In fact  $Mn^{2+}$  appeared to have significant inhibiting effect on total biomass, average thickness, maximum thickness and microcolony formation in  $\Delta sagS::CTX-sagS$  (Figure 3 and 4). Previous studies found that metals can both increase and inhibit biofilm formation which may account for why attachment is enhanced in  $\Delta sagS::CTX-sagS$  as  $Mn^{2+}$  may interact with SagS to increase attachment but in later stages may cause stress and inhibit biofilm formation (55–59). The effects  $Mn^{2+}$  has on SagS are very interesting and should be further investigated.

Next we performed a high throughput screen of potential compounds and initially found G6P, glycerol and  $\beta$ -methyl-D-galactosidase to have large enhancing effects on SagS-dependent biofilm attachment (Figure 5 and 6). To confirm the enhancing effects of these compounds we carried out further attachment assays in the presence of each compounds and found only G6P to consistently have enhanced attachment in only  $\Delta sagS::CTX-sagS$  but not  $\Delta sagS::CTX$  (Figure 6). This indicated that G6P enhances SagS-dependent biofilm formation. Further attachment assays at increasing concentrations of G6P showed that the effects this compound has on SagS-dependent attachment increases with increasing concentrations (Figure 7). Confocal microscopy and COMSTAT analysis of 3-day old biofilms revealed not only increased microcolony formation in treated  $\Delta sagS::CTX-sagS$  but also a significant increase in biomass, substratum thickness and increases in average and maximum thickness when compared to untreated  $\Delta sagS::CTX-sagS$ . While G6P did not have enhancing effects on biofilm formation in  $\Delta sagS::CTX$  (Figure 8 and 9). Our findings indicate that G6P is a ligand that enhances biofilm formation in *P. aeruginosa* by activating the SagS protein, which supports previous works that found exogenous glucose in EPS

to have enhancing effects on both biofilm formation and antibiotic resistance in *P. aeruginosa* (60).

In order to get a better understanding of how G6P impacts biofilm formation we next looked at how this compound effects the expression of biofilm marker genes *pslG* and *pelA* in 3-day old biofilms. Both of these genes are involved in exopolysaccharide production and are highly upregulated in biofilm form, with *pslG* playing a role in mannose-rich exopolysaccharides production and regulation of 3D microcolony structure and while *pelA* controls the production of glucose-rich extracellular matrix and regulation of initial biofilm attachment and formation (47, 48, 61, 62). We expected that if G6P acted as a signal that interacts with SagS to enhance biofilm formation and the biofilm phenotypes then these genes would have higher expression in treated  $\Delta sagS::CTX-sagS$  than in  $\Delta sagS::CTX$ . When both strains were normalized to their untreated counterpart G6P had increased gene expression in both strains. The  $\Delta sagS::CTX-sagS$  strain had a >2-fold increase in gene expression for both genes showing that G6P enhances biofilm formation. While  $\Delta sagS::CTX$  did have a >2-fold increase in gene expression in *pelA* there was only a very slight increase in gene expression in *pslG* (Figure 10). This revealed that while G6P had similar impacts in gene expression of *pelA* for both strains this compound had a very large increase in gene expression in only  $\Delta sagS::CTX-sagS$  for *pslG*. These results make sense as *pelA* helps to control initial attachment and biofilm formation, while *pslG* regulates 3D microcolony structures and as seen in Figure 8 confocal images,  $\Delta sagS::CTX-sagS$  had increased microcolony formation under G6P treated conditions, while  $\Delta sagS::CTX$  had very little microcolony formation in both conditions. In addition, both strains had formed monolayer biofilms which would account for why both strains had similar gene expression patterns for *pelA* (Figure 8 and 10). These results support that G6P stimulates SagS-dependent biofilm formation and enhances the biofilm phenotype by

increasing expression of the biofilm marker gene, *pslG*, in  $\Delta sagS::CTX-sagS$  but not  $\Delta sagS::CTX$ . Though further testing should be carried out to confirm these results, as only one trial was performed.

In all, our data strongly indicates that G6P enhances biofilm formation through activation of the SagS protein. These findings provide a better understanding of signals that promote biofilm formation and provide further insight into how SagS controls biofilm formation in *P. aeruginosa*. With the dangers that biofilms pose to human health understanding how signals promote biofilm formation can lead to more effective means of treating and preventing biofilms infections.

### **Future Directions**

While gene expression results for *pslG* seemed promising, further studies of other biofilm marker genes should be carried out as they could provide additional insight into how G6P contributes to the biofilm phenotype and SagS-dependent biofilm formation. The genes selected in this study both control EPS production, so selecting other biofilm marker genes like *anr*, which controls the 4-hydroxy-2-alkylquinoline-dependent quorum sensing pathway or *dnr*, which plays a role in regulating the reduction chain in anaerobic respiration, can help to provide a holistic view of how G6P impacts SagS-dependent biofilm formation (29, 48, 63, 64).

In addition, we plan to observe how G6P impacts the NicD protein in *P. aeruginosa* to gain a better understanding of how this molecule impacts SagS-dependent biofilm formation. This protein is a sensory diguanylate cyclase and helps to regulate biofilm formation and attachment, specifically dispersion, by controlling intracellular c-di-GMP levels. Utilizing a NicD *P. aeruginosa* mutant and growing it in the presence of G6P can reveal to us if this compound interacts with other sensory proteins that also control c-di-GMP levels or if it solely activates SagS.

With NicD being a protein that interacts with SagS, understanding if this compound interacts with NicD can provide further insight into how G6P stimulates SagS-dependent biofilm formation.

While our data indicates that G6P is a ligand that stimulates SagS-dependent biofilm formation we cannot say that this molecule directly interacts with SagS. This protein spans the inner membrane of *P. aeruginosa* with its sensory domain extending out into the periplasm (34). There is a possibility that G6P may not be able to get through the outer membrane, due to the phosphate group attached to it, to directly interact with SagS. Instead this molecule could indirectly activate SagS through osmotic stress or activating another protein which would then interact with SagS. Osmotic stress is a big driver of biofilm formation and it is common for sensory domains in bacteria to interact with other proteins in chemosensory systems, so both are possible (65, 66). Further studies such as crystalizing SagS in the presence of G6P for X-ray crystallography or a thermal shift assay may give more insight into if this ligand directly interacts with the active site of SagS.

## REFERENCES

1. Costerton JW, Lewandowski Z, Caldwell DE, Korber DR, Lappin-Scott HM. 1995. Microbial Biofilms. *Annu Rev Microbiol* 49:711–745.
2. Luppens SBI, Reij MW, Van der Heijden RWL, Rombouts FM, Abee T. 2002. Development of a standard test to assess the resistance of *Staphylococcus aureus* biofilm cells to disinfectants. *Appl Environ Microbiol* 8:e933.
3. Liao J, Schurr MJ, Sauera K. 2013. The merR-like regulator brlR confers biofilm tolerance by activating multidrug efflux pumps in *Pseudomonas aeruginosa* biofilms. *J Bacteriol* 195:3352–3363.
4. Liao J, Sauer K. 2012. The MerR-like transcriptional regulator BrlR contributes to *Pseudomonas aeruginosa* biofilm tolerance. *J Bacteriol* 194:4823–4836.
5. Jamal M, Ahmad W, Andleeb S, Jalil F, Imran M, Nawaz MA, Hussain T, Ali M, Rafiq M, Kamil MA. 2018. Bacterial biofilm and associated infections. *J Chinese Med Assoc*.
6. Bjarnsholt T. 2013. The role of bacterial biofilms in chronic infections. *APMIS Suppl* 121:1–51.
7. Irie Y, Borlee BR, O'Connor JR, Hill PJ, Harwood CS, Wozniak DJ, Parsek MR. 2012. Self-produced exopolysaccharide is a signal that stimulates biofilm formation in *Pseudomonas aeruginosa*. *Proc Natl Acad Sci U S A* 109:20632–20636.
8. Gupta P, Sarkar S, Das B, Bhattacharjee S, Tribedi P. 2016. Biofilm, pathogenesis and prevention—a journey to break the wall: a review. *Arch Microbiol*.
9. Rimondini L, Cochis A, Varoni E, Azzimonti B, Carrassi A. 2016. Biofilm formation on implants and prosthetic dental materials, p. 991–1027. *In Handbook of Bioceramics and Biocomposites*.
10. James GA, Swogger E, Wolcott R, Pulcini ED, Secor P, Sestrich J, Costerton JW, Stewart PS. 2008. Biofilms in chronic wounds. *Wound Repair Regen* 37–44.
11. McLaughlin-Borlace L, Stapleton F, Matheson M, Dart JKG. 1998. Bacterial biofilm on contact lenses and lens storage cases in wearers with microbial keratitis. *J Appl Microbiol* 84:827–838.
12. Faure E, Kwong K, Nguyen D. 2018. *Pseudomonas aeruginosa* in Chronic Lung Infections: How to Adapt Within the Host? *Front Immunol*.
13. Estahbanati HK, Kashani PP, Ghanaatpisheh F. 2002. Frequency of *Pseudomonas aeruginosa* serotypes in burn wound infections and their resistance to antibiotics. *Burns* 28:340–348.
14. Lyczak JB, Cannon CL, Pier GB. 2002. Lung infections associated with cystic fibrosis. *Clin Microbiol Rev*.
15. Heijerman H. 2005. Infection and inflammation in cystic fibrosis: A short review. *J Cyst Fibros* 2:3–5.
16. Karatan E, Watnick P. 2009. Signals, Regulatory Networks, and Materials That Build and Break Bacterial Biofilms. *Microbiol Mol Biol Rev* 61:322–332.
17. Park A, Jeong HH, Lee J, Kim KP, Lee CS. 2011. Effect of shear stress on the formation of bacterial biofilm in a microfluidic channel. *Biochip J* 5:236–241.
18. Prigent-Combaret C, Brombacher E, Vidal O, Ambert A, Lejeune P, Landini P, Dorel C. 2001. Complex regulatory network controls initial adhesion and biofilm formation in *Escherichia coli* via regulation of the *csqD* gene. *J Bacteriol* 183:7213–7223.

19. O'Toole GA, Kolter R. 1998. Initiation of biofilm formation in *Pseudomonas fluorescens* WCS365 proceeds via multiple, convergent signalling pathways: A genetic analysis. *Mol Microbiol* 28:449–461.
20. Stanley NR, Lazazzera BA. 2004. Environmental signals and regulatory pathways that influence biofilm formation. *Mol Microbiol*.
21. Hernandez ME, Newman DK. 2001. Extracellular electron transfer. *Cell Mol Life Sci*.
22. González-Pastor JE, Hobbs EC, Losick R. 2003. Cannibalism by sporulating bacteria. *Science* (80- ) 301:510–513.
23. Capra EJ, Laub MT. 2012. Evolution of Two-Component Signal Transduction Systems. *Annu Rev Microbiol* 66:325–347.
24. Stock AM, Robinson VL, Goudreau PN. 2000. Two-Component Signal Transduction. *Annu Rev Biochem* 25–51.
25. Gao R, Mack TR, Stock AM. 2007. Bacterial response regulators: versatile regulatory strategies from common domains. *Trends Biochem Sci*.
26. Mitrophanov AY, Groisman EA. 2008. Signal integration in bacterial two-component regulatory systems. *Genes Dev*.
27. Petrova OE, Sauer K. 2011. SagS contributes to the motile-sessile switch and acts in concert with BfiSR to enable *Pseudomonas aeruginosa* biofilm formation. *J Bacteriol* 193:6614–6628.
28. Petrova OE, Gupta K, Liao J, Goodwine JS, Sauer K. 2017. Divide and conquer: the *Pseudomonas aeruginosa* two-component hybrid SagS enables biofilm formation and recalcitrance of biofilm cells to antimicrobial agents via distinct regulatory circuits. *Environ Microbiol* 19:2005–2024.
29. Dingemans J, Poudyal B, Sondermann H, Sauer K. 2018. The Yin and Yang of SagS: Distinct Residues in the HmsP Domain of SagS Independently Regulate Biofilm Formation and Biofilm Drug Tolerance. *mSphere* 3:e00192–00118.
30. Dingemans J, Al-Feghali RE, Sondermann H, Sauer K. 2019. Signal Sensing and Transduction Are Conserved between the Periplasmic Sensory Domains of BifA and SagS. *mSphere* e00442-19.
31. Gupta K, Marques CNH, Petrova OE, Sauer K. 2013. Antimicrobial tolerance of *Pseudomonas aeruginosa* biofilms is activated during an early developmental stage and requires the two-component hybrid SagS. *J Bacteriol* 195:4975–87.
32. Dingemans J, Al-Feghali RE, Lau GW, Sauer K. 2019. Controlling chronic *Pseudomonas aeruginosa* infections by strategically interfering with the sensory function of SagS. *Mol Microbiol* 111:1211–1228.
33. Petrova OE, Sauer K. 2009. A novel signaling network essential for regulating *Pseudomonas aeruginosa* biofilm development. *PLoS Pathog* 5:e1000668.
34. Petrova OE, Sauer K. 2010. The novel two-component regulatory system BfiSR regulates biofilm development by controlling the small RNA rsmZ through CafA. *J Bacteriol* 192:5275–5288.
35. Gupta K, Liao J, Petrova OE, Cherny KE, Sauer K. 2014. Elevated levels of the second messenger c-di-GMP contribute to antimicrobial resistance of *Pseudomonas aeruginosa*. *Mol Microbiol* 92:488–506.
36. D'Argenio DA, Miller SI. 2004. Cyclic di-GMP as a bacterial second messenger. *Microbiology*.
37. Davey ME, O'toole GA. 2000. *Microbial Biofilms: from Ecology to Molecular Genetics*.

- Microbiol Mol Biol Rev 64:847–867.
38. Mann EE, Wozniak DJ. 2012. *Pseudomonas* biofilm matrix composition and niche biology. FEMS Microbiol Rev.
  39. Shirtliff M LJ. 2009. The role of biofilms in device-related infections. Springer.
  40. Heydorn A, Nielsen AT, Hentzer M, Sternberg C, Givskov M, Ersboll BK, Molin S. 2000. Quantification of biofilm structures by the novel computer program COMSTAT. Microbiology 146:2395–2407.
  41. Göpel Y, Görke B. 2018. Interaction of lipoprotein QseG with sensor kinase QseE in the periplasm controls the phosphorylation state of the two-component system QseE/QseF in *Escherichia coli*. PLoS Genet 14:e1007547.
  42. Livak KJ, Schmittgen TD. 2001. Analysis of relative gene expression data using real-time quantitative PCR and the 2- $\Delta\Delta$ CT method. Methods 25:402–408.
  43. Mhatre E, Troszok A, Gallegos-Monterrosa R, Lindstädt S, Hölscher T, Kuipers OP, Kovács ÁT. 2016. The impact of manganese on biofilm development of *Bacillus subtilis*. Microbiol (United Kingdom) 162:1468–1478.
  44. Shemesh M, Chaia Y. 2013. A combination of glycerol and manganese promotes biofilm formation in *Bacillus subtilis* via histidine kinase KinD signaling. J Bacteriol 195:2747–2754.
  45. Das T, Sehar S, Koop L, Wong YK, Ahmed S, Siddiqui KS, Manefield M. 2014. Influence of calcium in extracellular DNA mediated bacterial aggregation and biofilm formation. PLoS One 9:e91935.
  46. Sauer K, Camper AK, Ehrlich GD, Costerton JW, Davies DG. 2002. *Pseudomonas aeruginosa* displays multiple phenotypes during development as a biofilm. J Bacteriol 184:1140–1154.
  47. Goodman AL, Kulasekara B, Rietsch A, Boyd D, Smith RS, Lory S. 2004. A signaling network reciprocally regulates genes associated with acute infection and chronic persistence in *Pseudomonas aeruginosa*. Dev Cell 7:745.
  48. Dingemans J, Monsieurs P, Yu SH, Crabbé A, Förstner KU, Malfroot A, Cornelis P, Van Houdt R. 2016. Effect of shear stress on *Pseudomonas aeruginosa* isolated from the cystic fibrosis lung. MBio 7:e00813–e00816.
  49. Fazli M, Almblad H, Rybtke ML, Givskov M, Eberl L, Tolker-Nielsen T. 2014. Regulation of biofilm formation in *Pseudomonas* and *Burkholderia* species. Environ Microbiol.
  50. Sakuragi Y, Kolter R. 2007. Quorum-sensing regulation of the biofilm matrix genes (pel) of *Pseudomonas aeruginosa*. J Bacteriol 189:5383–5386.
  51. Nadal Jimenez P, Koch G, Thompson JA, Xavier KB, Cool RH, Quax WJ. 2012. The Multiple Signaling Systems Regulating Virulence in *Pseudomonas aeruginosa*. Microbiol Mol Biol Rev 76:46–65.
  52. Francis VI, Stevenson EC, Porter SL. 2017. Two-component systems required for virulence in *Pseudomonas aeruginosa*. FEMS Microbiol Lett.
  53. Valentini M, Filloux A. 2016. Biofilms and Cyclic di-GMP (c-di-GMP) signaling: Lessons from *Pseudomonas aeruginosa* and other bacteria. J Biol Chem.
  54. Upadhyay AA, Fleetwood AD, Adebali O, Finn RD, Zhulin IB. 2016. Cache Domains That are Homologous to, but Different from PAS Domains Comprise the Largest Superfamily of Extracellular Sensors in Prokaryotes. PLoS Comput Biol 12:e1004862.
  55. Jansen E, Michels M, van Til M, Doelman P. 1994. Effects of heavy metals in soil on microbial diversity and activity as shown by the sensitivity-resistance index, an ecologically



- relevant parameter. *Biol Fertil Soils* 17:177–184.
56. Kaplan JB, Izano EA, Gopal P, Karwacki MT, Kim S, Bose JL, Bayles KW, Horswill AR. 2012. Low levels of  $\beta$ -Lactam antibiotics induce extracellular DNA release and biofilm formation in *Staphylococcus aureus*. *MBio* 1–14.
  57. Hennequin C, Aumeran C, Robin F, Traore O, Forestier C. 2012. Antibiotic resistance and plasmid transfer capacity in biofilm formed with a CTX-M-15-producing *Klebsiella pneumoniae* isolate. *J Antimicrob Chemother* 2123–2130.
  58. Navarrete F, De La Fuente L. 2014. Response of *Xylella fastidiosa* to zinc: Decreased culturability, increased exopolysaccharide production, and formation of resilient biofilms under flow conditions. *Appl Environ Microbiol* 97–107.
  59. Jomova K, Valko M. 2011. Advances in metal-induced oxidative stress and human disease. *Toxicology*.
  60. She P, Wang Y, Liu Y, Tan F, Chen L, Luo Z, Wu Y. 2019. Effects of exogenous glucose on *Pseudomonas aeruginosa* biofilm formation and antibiotic resistance. *Microbiologyopen* e933.
  61. Wei Q, Ma LZ. 2013. Biofilm matrix and its regulation in *Pseudomonas aeruginosa*. *Int J Mol Sci*.
  62. Ma L, Conover M, Lu H, Parsek MR, Bayles K, Wozniak DJ. 2009. Assembly and development of the *Pseudomonas aeruginosa* biofilm matrix. *PLoS Pathog* 3:e1000354.
  63. Crespo A, Pedraz L, Astola J, Torrents E. 2016. *Pseudomonas aeruginosa* exhibits deficient biofilm formation in the absence of class II and III ribonucleotide reductases due to hindered anaerobic growth. *Front Microbiol* 7:688.
  64. Hammond JH, Dolben EF, Smith TJ, Bhujju S, Hogan DA. 2015. Links between Anr and quorum sensing in *Pseudomonas aeruginosa* biofilms. *J Bacteriol* 197:2810–2820.
  65. Li S, Liang H, Wei Z, Bai H, Li M, Li Q, Qu M, Shen X, Wang Y, Zhang L. 2019. An osmoregulatory mechanism operating through OmpR and LrhA controls the motilesessile switch in the plant growth-promoting bacterium *Pantoea alhagi*. *Appl Environ Microbiol* 85:e00077–19.
  66. Glekas GD, Mulhern BJ, Kroc A, Duelfer KA, Lei V, Rao C V., Ordal GW. 2012. The *Bacillus subtilis* chemoreceptor McpC senses multiple ligands using two discrete mechanisms. *J Biol Chem* 287:39412–39418.